ELSEVIER

Journal of Atmospheric and Solar-Terrestrial Physics 67 (2005) 1321–1330

Journal of ATMOSPHERIC AND SOLAR-TERRESTRIAL PHYSICS

www.elsevier.com/locate/jastp

# Sensitivity of solar UV radiation to ozone and temperature profiles at Thessaloniki (40.5°N, 23°E), Greece

A. Kazantzidis[a,*], A.F. Bais[a], D.S. Balis[a], E. Kosmidis[a], C.S. Zerefos[b]

[a]*Laboratory of Atmospheric Physics, Campus Box 149, Aristotle University of Thessaloniki, 54124 Thessaloniki, Greece*
[b]*Laboratory of Climatology and Atmospheric Environment, Faculty of Geology, University of Athens, 15784 Athens, Greece*

Received 12 August 2004; received in revised form 13 May 2005; accepted 28 May 2005
Available online 21 July 2005

**Abstract**

Measured ozone and temperature vertical profiles from Thessaloniki, Greece, were used together with the mid-latitude standard profiles as input data in a radiative transfer model. Calculations of direct and global solar irradiance, actinic flux, UV-B and CIE weighted integrals for solar zenith angles of 30°, 70° and 85° were performed and analyzed. Variable temperature values and ozone redistribution may change UV radiation reaching the surface significantly more than the proposed measurement uncertainties for high solar zenith angles. A specific measured profile corresponding to air masses of polar origin probed over Thessaloniki was selected and the differences in vertical distribution of UV-B radiation were discussed. Obtained results revealed that the use of an inappropriate temperature and ozone profile may lead to significant changes at small UV-B wavelengths and high solar zenith angles. In this case, the use of seasonal average vertical profiles of ozone and temperature for a given area may be carefully utilized when accurate model spectral calculations are needed and comparison with measurements in the troposphere performed.


*Keywords:* UV radiation; Ozone profile; Modeling

## 1. Introduction

The relationship between ultraviolet radiation measured at the surface and total ozone, aerosol properties, clouds and surface albedo has been discussed in detail in Bais et al. (1993), Booth and Madronich (1994), Kazantzidis et al. (2001), Kerr and McElroy (1993), Kylling et al. (1998), McKenzie et al. (1991), Fioletov et al. (1997), Zerefos et al. (1997, 1998, 2000). Radiative transfer models for ultraviolet radiation are available (Madronich, 1993; Ruggaber et al., 1994; Mayer et al., 1997) and have been widely used in recent years for interpreting these UV measurements (e.g. Bais et al., 2001; Kylling et al., 2000a, b; Kylling and Mayer, 2001; Mayer et al., 1997, 1998; Weihs and Webb, 1997a; Zeng et al., 1994). Results from these studies suggest that model calculations in most cases can reproduce UV irradiance with uncertainties comparable to those of the measurements. Radiative transfer models have been also used to estimate UV levels at locations where measurements are not available (Mayer et al., 1998), or for UV forecasting (Koepke et al., 1998; De Backer et al., 2001; Balis et al., 2002).

The quality of results of UV models depends on the accuracy of the radiative transfer algorithm used (e.g. Mayer et al., 1997), as well as on the accuracy of the atmospheric parameters, which are needed as inputs to the models (e.g. Forster, 1995; Schwander et al., 1997;

*Corresponding author. Tel.: +302310998049; fax: +202310998090.
*E-mail address:* akaza@auth.gr (A. Kazantzidis).

1364-6826/$ - see front matter 
doi:10.1016/j.jastp.2005.05.003

Weihs and Webb, 1997b). Those papers present sensitivity studies by perturbing the standard vertical atmospheric profiles of ozone and temperature and suggest that significant differences are introduced, which increase strongly with solar zenith angle and inversely with wavelength. The considerable effect of ozone redistribution from the stratosphere and the troposphere on UV radiation was shown by Bruehl and Crutzen (1989) and Tsay and Stamnes (1992). Using selected cases, the effects of ozone redistribution from the stratosphere to the troposphere, the difference in tropopause and ozonepause heights and the importance of the shape of the ozone profile were discussed by Lapeta et al. (2000). As it was reported, the replacement of US standard vertical profile by a measured one induces changes in model calculated erythemal dose up to 12%. In addition, discrepancies of about 3% were reported as a result of using different ozone cross-sections, which are in agreement with the results from Bais et al. (2003). McKenzie et al. (2003) presented a climatology of ozone profiles measured in Lauder, New Zealand and Hohenpeissenberg, Germany for the period 1987–1991 and reported that the contribution of tropospheric and lower stratospheric ozone is larger in Europe, affecting erythemally weighted UV by 1–2% and DNA-weighted irradiance by 2–3%.

In this study, measured ozone and temperature profiles at Thessaloniki, Greece, are used as input data to a radiative transfer model, in order to examine their influence on model calculated direct and global irradiance, actinic flux and integrals of UV-B and CIE weighted irradiances reaching the surface with respect to model calculations based on standard profiles. A special case corresponding to air masses of polar origin over Thessaloniki is presented more extensively and the calculated differences in vertical profiles of solar radiation quantities are discussed.

## 2. Vertical atmospheric and ozone profiles

Scientists from the Laboratory of Atmospheric Physics, Thessaloniki, Greece (40.5°N, 23°E), launched 40 ozonesondes over the period 1994–1997 in the framework of the projects SESAME (e.g. Rex et al., 1999), PAUR (e.g. Zerefos et al., 2002) and SUSPEN (e.g. Bais et al., 2001). Most of the measurements (32) of the vertical profile of ozone and temperature were performed during winter (December–mid-March), while 8 ozonesondes were launched during summer period (June and July). In all cases, ECC-sondes were used and launches were performed at the "Macedonia" airport of Thessaloniki, following the preparation rules of the manufacturer and using the facilities of the airport radiosonde station. According to WMO (1998), the accuracy of the ECC-sondes is better than ±5% in the lower to middle stratosphere (from the tropopause to 28 km altitude). In the troposphere, systematic differences of ±5–10% are reported. For temperature profiles the uncertainty is within ±1% at all altitudes (Kerr et al., 1994).

Measured vertical profiles of ozone and temperature were compared with the Air Force Geophysical Laboratory (AFGL) standard profiles (Anderson et al., 1986). For winter and summer period the corresponding mid-latitude standard profiles were used for comparison. Percentage differences between summer and winter ozone vertical standard profiles (normalized to the same total ozone column 300 D.U.) reach 50%, mainly because of the redistribution of ozone to higher altitudes during summer. Mean temperature difference between the two standard profiles is 11.7 K. Standard profiles are often used for model calculations of solar UV irradiance, since usually only measurements of the total ozone amount are available and not its vertical distribution.

Averaged difference and standard deviation in 5 km steps between all measured profiles of ozone and temperature and the corresponding AFGL profiles for mid-latitude summer and winter are presented in Table 1. Measured ozone profiles were scaled to the AFGL total ozone column in order to examine only the difference in profile shape and possible ozone redistribution and not in ozone column values. Results above 35 km are not presented, since most of the balloons were burst at these altitudes. However, constant mixing ratio for atmospheric species have used above 35 km in model calculations. Comparisons reveal that, measured ozone at Thessaloniki in the lower troposphere (0-5 km) is in most cases higher than the AFGL standard (e.g. Kourtidis et al., 2002; Galani et al., 2003). In contrast, lower ozone values are measured in the upper troposphere and the lower stratosphere (5–20 km). Absolute differences within 5.5 K are calculated also in temperature values (Table 1), corresponding to percentage differences close to the proposed uncertainty of

Table 1
Average difference and standard deviation in 5 km steps between the 40 measured profiles of ozone (percentage values) and temperature (absolute values) at Thessaloniki and the corresponding AFGL profiles for mid-latitude summer and winter

| Height (km) | $\Delta O_3/O_{3(standard)}$ (%) | $\Delta T$ |
|---|---|---|
| 0–5 | 61 ± 38 | 5.5 ± 4.8 |
| 6–10 | −17 ± 23 | −0.13 ± 4.3 |
| 11–15 | −37 ± 26 | −2.6 ± 4.0 |
| 16–20 | −10 ± 15 | −3.9 ± 3.3 |
| 21–25 | 11 ± 12 | −1.8 ± 3.0 |
| 26–30 | 11 ± 15 | 2.5 ± 5.4 |
| 31–35 | 16 ± 15 | 1.6 ± 4.5 |

measurements ($\pm 1\%$, Kerr et al., 1994). It should be mentioned that the scope of this paper is not a detailed analysis of the differences between measured and standard vertical profiles at Thessaloniki, but to examine the possible effects on the calculated transmission of UV radiation through the atmosphere.

## 3. Model description

In this study, the Tropospheric Ultraviolet and Visible (TUV) Version 4.0 model was used (Madronich, 1993). The radiative transfer equation is solved with the discrete ordinates algorithm (Stamnes et al., 1988), using six streams and pseudospherical correction (Dahlback and Stamnes, 1991). Calculations of direct and global solar irradiance on a horizontal surface and actinic flux from 290 to 400 nm were performed with 1 nm steps and resolution. UV-B and CIE weighted integrals (McKinlay and Diffey, 1987) were also calculated.

The Atlas 3 spectrum (shifted to air-wavelengths) was used as an extraterrestrial solar flux. All model calculations were performed with standard aerosol optical depth (0.38 at 340 nm with Angstrom $\alpha$exponent coefficient of 1.5), assuming the vertical profile by Elterman (1968). Single scattering albedo and asymmetry parameter of 0.88 and 0.7, respectively at 340 nm, were considered as typical for Thessaloniki and assumed constant with wavelength, altitude and relative humidity (Bais et al., 2004). The model used for ozone absorption the cross-sections by Bass and Paur (1985) and for Rayleigh scattering those calculated according to the analytical function of Nicolet (1984). Surface albedo of 0.03 was assumed constant for the entire UV region, following the suggestions by Blumthaler and Ambach (1988). The measured and the AFGL for mid-latitude summer and winter vertical profiles were used in model calculations, interpolated in 1 km altitude increments. Vertical profiles of ozone were scaled to the mean total ozone measured at the same day, either by a Brewer spectrophotometer operating regularly at the Laboratory of Atmospheric Physics, or by the total ozone mapping spectrometer (TOMS). The total ozone values for the ozone profiles used in this study were in the range of 287–423 DU. The respective AFGL profiles for air molecule number density were used in all model calculations, scaled to the measured sea level pressure for all ozone soundings.

## 4. Effect of vertical ozone and temperature profiles on surface UV radiation

In order to estimate the effect of vertical profiles on UV radiation reaching the ground, direct and global irradiance, actinic flux, UVB and CIE erythemal doses were calculated twice using ozone and temperature profiles from LAP dataset.

In Fig. 1 the ratios of the calculated direct solar UV irradiance at zenith angles of 30° and 70° are presented. From the total number of 40 vertical profiles, the first 32 were measured during winter, while the rest during summer. For wavelengths higher than 305 nm modeled values agree within $\pm 3\%$ for both solar zenith angles. On the contrary, model calculations at 295 nm using the measured profiles deviate up to 8%. Since, direct solar irradiance is unaffected by ozone profile changes, such differences could be attributed to the dependence of ozone absorption from wavelength and temperature. Values of ozone absorption cross-section by Bass and Paur (1985) increase with temperature (values for 263 K are 5% and 10% higher at 300 and 310 nm, respectively compared to those at for 226 K) and decrease significantly with wavelength (cross-sections are four times

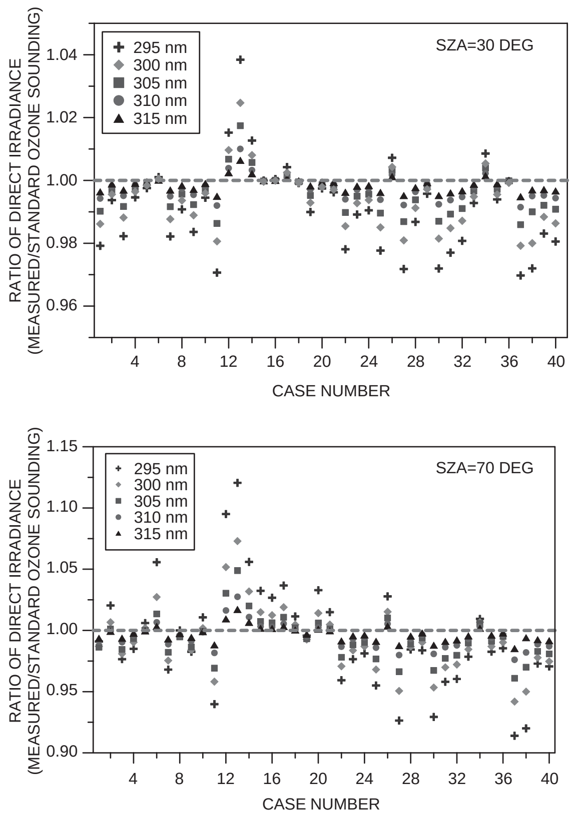


Fig. 1. Ratios of model calculated direct solar irradiance at five UV-B wavelengths for solar zenith angles of 30° (upper panel) and 70° (lower panel) using the 40 ozone and temperature measured profiles from LAP dataset (case number) and the corresponding mid-latitude summer and winter AFGL profiles. From the total number of 40 vertical profiles, the first 32 were measured during winter, while the rest during summer.

smaller at 310 nm compared with values at 300 nm) in UV-B part of solar spectrum.

In Fig. 2, ratios of modeled solar actinic flux using measured and standard vertical profiles are presented for three solar zenith angles (30°, 70° and 85°). For 30° and 70°, the differences increase significantly at shorter wavelengths, where the use of measured profiles generally underestimates actinic flux (with some exceptional cases at 30°). Differences in actinic flux up to 5% at 305 nm and 15% at 295 nm are calculated at 30°, while underestimation reaches 7% and 40%, respectively at 70°. Apart from affecting the ratios by changes in direct component of solar radiation, it has to be noted that (except of some low-numbered cases in LAP dataset) the measured ozone content at lower troposphere altitudes is more than the proposed by standard profiles (Table 1). This kind of ozone redistribution (it will be discussed in detail later in this study) leads to underestimation of actinic flux at 70°, where scattered solar radiation penetrates the enhanced ''optical path'' in the troposphere (e.g. Bruehl and Crutzen, 1989). At 85° the differences in actinic flux become significant even for higher UV-B wavelengths. However, reverse results have been calculated in some cases during summer (case numbers higher than 32). It has been shown by Lapeta et al. (2000), that the decreased temperature profile values could lead to increase of solar UV radiation at the surface, although the existence of ozone redistribution from the stratosphere to the troposphere. As an example, the combination of increased proportion of tropospheric ozone (110% higher than the standard value in the lower troposphere) with significantly lower temperature values (by 18 K in the troposphere and 9 K close to the ozonopause) in case number 38 increases UV irradiance at 310 nm by 27%. The corresponding changes in global irradiance differ by ±2% at 30° and 70° for the according cases for actinic fluxes, because of the different contribution of diffuse radiation on each radiative quantity. However, for the solar zenith angle of 85°, where the diffuse component is dominant, differences with respect to the actinic flux are generally within 4%, while for case number 38 reach 10%.

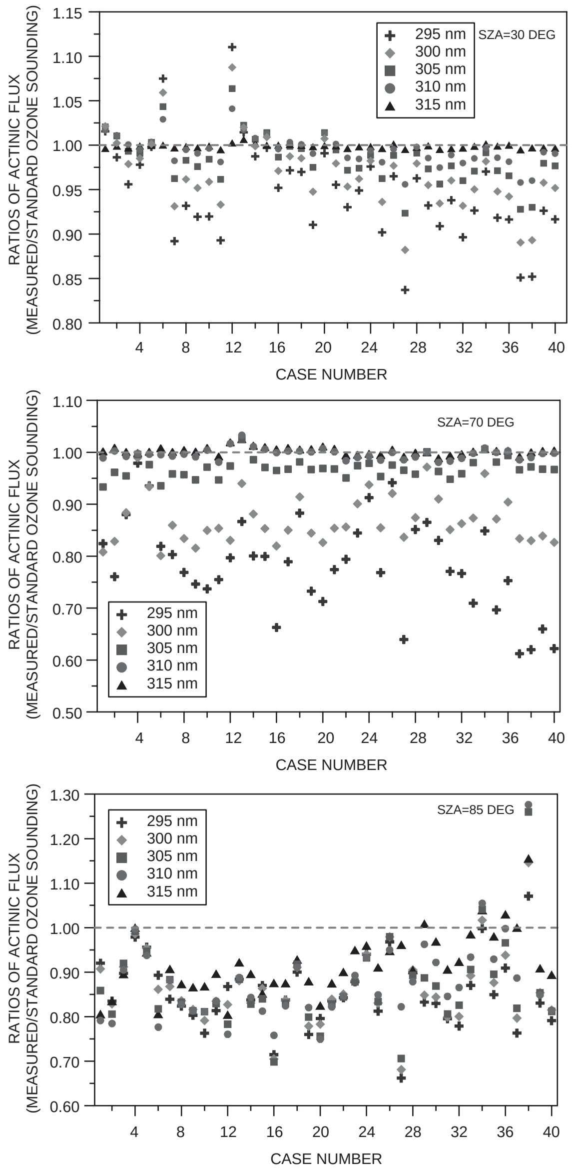


Fig. 2. Ratios of model calculated solar actinic flux at five UV-B wavelengths for solar zenith angles of 30° (upper panel), 70° (middle panel) and 85° (lower panel) using the 40 ozone and temperature measured profiles from LAP dataset (case number) and the corresponding standard profiles.

Finally, differences of UV-B and CIE erythemal dose within 3%, respectively, are calculated for 30° and 70° using the measured and standard profiles (Fig. 3). The profile effect on short UV-B wavelengths (where

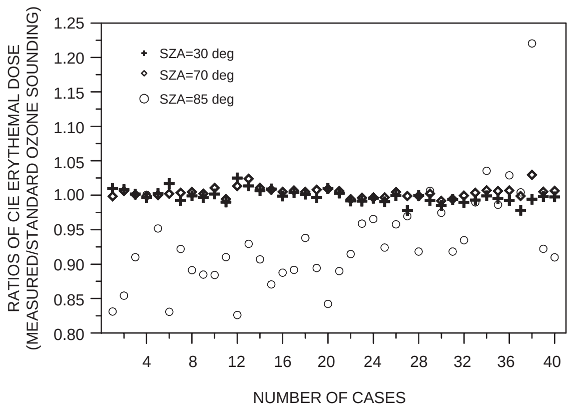


Fig. 3. Ratios of model calculated CIE erythemal dose for solar zenith angles of 30°, 70° and 85°, using the measured and standard profiles for ozone and temperature.

irradiances are low) it is not straightforward to integrated values, so differences of this magnitude could be reasonably accepted. However, for 85°, the significant differences on calculated irradiance at higher UV-B wavelengths results in changes within 20% in erythemal UV doses. These changes are higher than those proposed by Lapeta et al., 2000 (12%) for 50 temperature and ozone profile pairs measured in Legionowo, Poland in period 1979–1997. For 85°, the modeled UV-B dose calculations using the standard and the measured vertical profiles are different by up to 10% with respect to the CIE changes.

Above-mentioned differences in model derived radiative quantities indicate that for accurate spectral model calculations and for comparison with high-quality spectral ground-based measurements the vertical profile of temperature values and the distribution of ozone must be well known, especially for high solar zenith angles.

## 5. Effect of ozone and temperature profile on vertical distribution of UV radiation

As shown in previous section, although standard ozone and temperature profiles are often used in model calculations usually due to lack of measurements, considerable percentage differences could be observed especially at short UV-B wavelengths. In this section, one measured profile is selected in an attempt to examine the single effect of ozone and temperature profile and the differences on the vertical distribution of UV radiation.

Case 13 corresponds to an ozone sounding performed at 28 January 1995. The daily mean of total ozone was 300 DU and the balloon burst altitude was 31 km. The measured and standard vertical profiles of ozone and temperature are presented in Figs. 4a and 4b, respectively. It is revealed that there are significant differences in ozone distribution and in temperature values with altitude. It seems that there is a redistribution of ozone to lower heights, with the measured profile having +10 DU below 6 km, −47 DU between 6 and 17 km and +35 DU between 18 and 27 km, resulting in substantial changes of UV-B transmission. In addition, measured temperature is higher by almost ~5 K in the troposphere and lower by ~25 K in the lower stratosphere. Back-trajectories analysis for 10 days (Fig. 4c) in the frame of SESAME project (Knudsen and Carver, 1994) reveals that during that day air masses of polar origin were probed over Thessaloniki. Model calculated differences in direct and global solar irradiance and actinic flux at 300 nm reaching the surface, using the measured and the standard vertical profiles of ozone and temperature, are presented for 30° and 70° in Table 2. According to results, the use of the measured profiles increases direct solar irradiance for both solar zenith angles. However, calculated global irradiance and actinic flux are decreased for 70°.

Ratios of the model calculated vertical distribution for direct, global irradiance and actinic flux using measured and standard profiles are presented in Figs. 5 and 6. Measured and standard ozone profiles and the measured temperature profile were used as input data in TUV model and the ratio of the two calculated profiles of radiation is presented graphically in order to examine the ozone significance (effect of ozone). Measured and standard temperature profiles and the measured ozone profile were used as model input data and the single effect of temperature is also presented (effect of temperature). Finally, model calculations using the measured and the standard profiles of ozone and temperature are compared (combined effect).

Model direct irradiance (at 300 nm) ratios with altitude using the measured and standard profiles of ozone and temperature for 30° and 70° are presented in Fig. 5. Temperature profile effect is dominant on model-calculated differences, decreasing (increasing) direct irradiance in cases of lower (higher) values (relative to the AFGL profile) by −2% (+3.5%). For 70° (Fig. 5, lower panel), the effect is stronger, so model calculations differ from −4% up to +10.5% due to the enhanced optical path of direct solar radiation. The lower measured temperature values induce for 70° significant positive change in direct irradiance between 5 and 25 km. On the contrary, the presence of more ozone content and higher temperature decrease the ratio below 5 km.

Although, the temperature effect on vertical profile of actinic flux and global irradiance induce changes up to 5% and 8% at 300 nm for 30° and 70°, respectively, the ozone effect is dominant (Fig. 6).

For 30° (Fig. 6, upper panel), the increase of ozone content above 15 km does not affect significantly both radiation quantities. According to model calculations the direct part of them at these altitudes is of most importance representing at 15 km, 89% of actinic flux and 93% of global irradiance. In this case, the effect of temperature on direct irradiance is also evident on radiation quantities. On the contrary, the ozone reduction between 5 and 15 km increase the actinic flux and the global irradiance ratio to 11% and 6.5%, respectively. Most of this enhancement is “covered”, because of strong solar radiation absorption inside the rich ozone layer below 5 km. Differences in variation between actinic flux and global irradiance can be attributed to its increased percentage of diffuse part, modifying the results of the above-described phenomenon. Model derived diffuse part of solar radiation becomes more important representing 34% of actinic flux and 22% of global irradiance at 8 km and 73% and 63%, respectively at the ground.

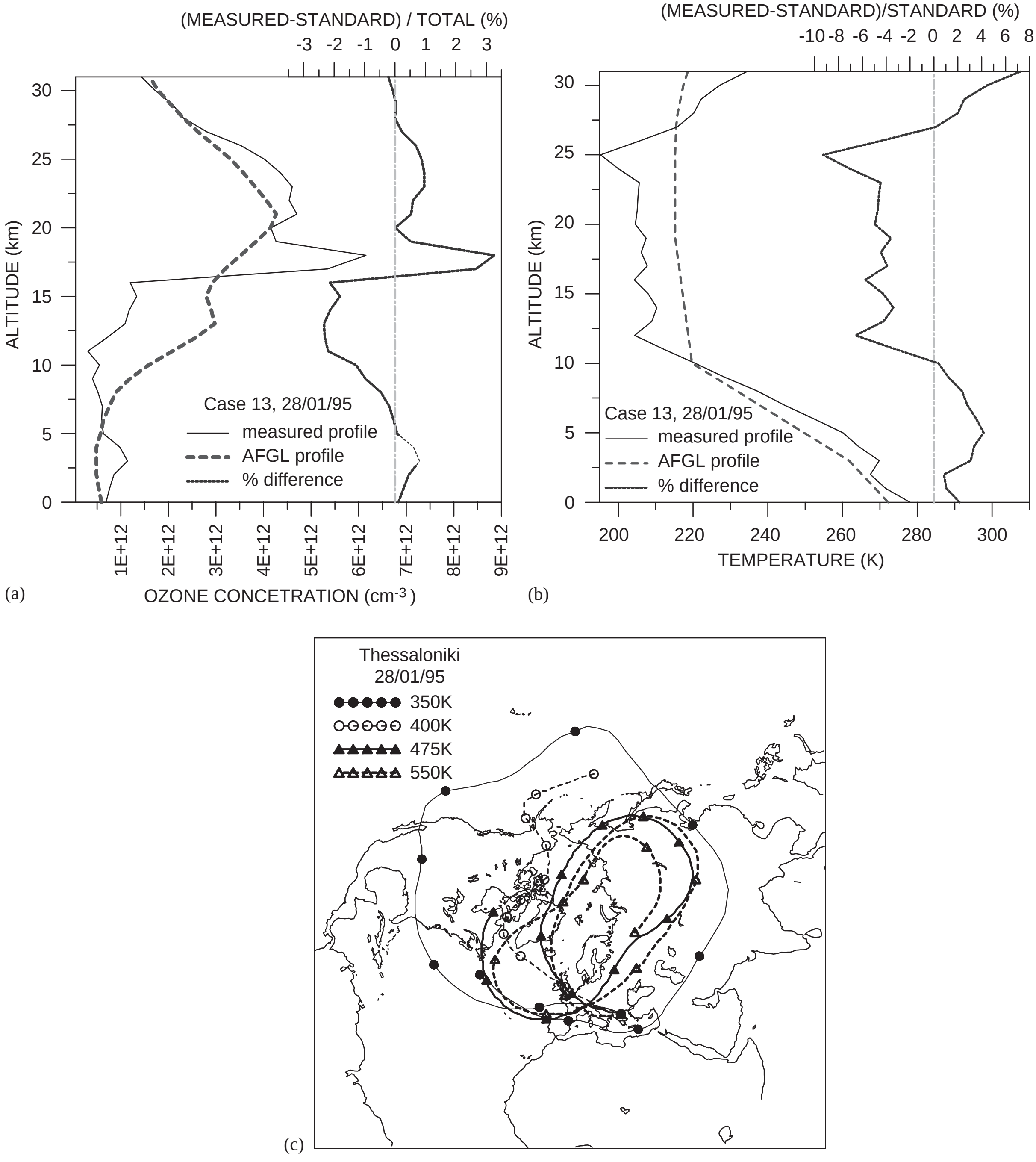


Fig. 4. (a) The measured and standard AFGL vertical profiles of ozone at 28/01/1995 (case 13). Percentage difference between profiles divided with total ozone column value is also presented (right); (b) the measured and standard AFGL vertical profiles of temperature at 28/01/1995 (case 13). Percentage difference between profiles is also presented (right); (c) analytical back trajectories of air masses at different temperature levels at Thessaloniki for 28/01/1995. Each dot in the figure corresponds to one-day time interval.

For 70° (Fig. 6, lower panel), the calculated differences ($\pm 5\%$) in ratios of global irradiance and actinic flux above 19 km could be mainly attributed to the significant differences of vertical temperature profiles. When ozone increases below, weakening of diffuse radiation causes decrement of global irradiance and actinic flux values (e.g. Schwander et al., 1997). The calculated stronger decrease of global irradiance should

Table 2
Differences in direct and global solar irradiance and actinic flux reaching the surface, when using the measured vertical profiles of ozone and temperature at 28 January 1995 instead of the standard AGFL winter mid-latitude profile

| Solar zenith angle (°) | Direct irradiance (%) | Actinic flux (%) | Global irradiance (%) |
|---|---|---|---|
| 30 | +2.5 | +2 | +2.5 |
| 70 | +7.3 | −6 | −6 |

Results are presented for 300 nm and for two solar zenith angles (30° and 70°).

be expected, since it is influenced by diffuse radiation more than the actinic flux. In the lower troposphere the diffuse component of solar radiation is increased and more scattered, so there are more photons coming from high polar angles and penetrating longer optical paths. As a result, the actinic flux is still reduced by 6% below 8 km. According to model results, decreases of ~17% for global irradiance and 5–15% for actinic flux are calculated in the troposphere when using the measured ozone profile.

The ratio of model calculations at two solar zenith angles for the shorter part of UV-B range that reaches surface using the measured and the standard vertical profiles of ozone and temperature (Fig. 1) revealed that the above presented results for 70 degrees at 300 nm are not representative for all UV-B wavelengths. The same analysis for 310 nm and for 70° is presented in Fig. 7 and the calculated differences are less significant. In this case, the use of measured instead of the standard vertical profiles in model calculations fairly increase (~3%) the global irradiance and actinic flux at the ground and affects their variation with altitude in a different way. This reverse result can be explained by the decreased ozone absorption and the increased percent of direct component in global irradiance and actinic flux at longer UV-B wavelengths. In general, the use of the standard vertical profiles of ozone and temperature as input data in model spectral calculations of the vertical distribution of UV radiation may produce non-satisfactory results for small UV-B wavelengths and high solar zenith angles.

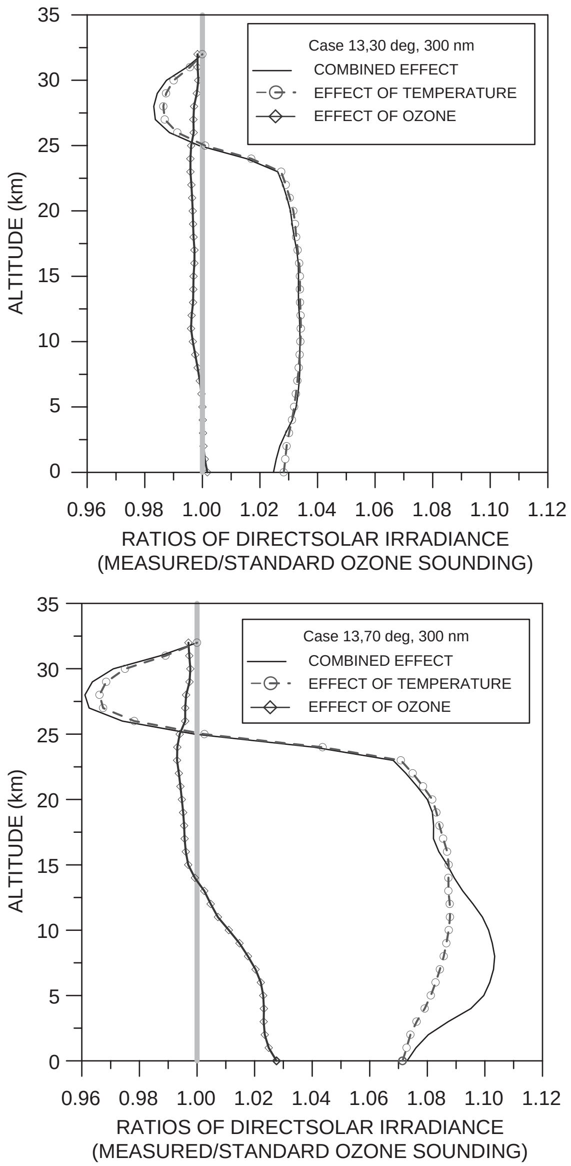


Fig. 5. Model calculated ratios of direct solar irradiance for 300 nm with altitude using the measured and standard ozone and temperature profiles at 30° (upper panel) and 70° (lower panel).

## 6. Conclusions

Measured ozone and temperature vertical profiles at Thessaloniki, Greece and the corresponding mid-latitude standard AFGL profiles, were used as model input parameters in order to estimate the effect on radiative transfer calculated UV-B solar radiation reaching the ground at zenith angles of 30°, 70° and 85°. Because of different temperature profiles, changes for direct irradiance at 295 nm up to 4% and 12% were calculated for both solar zenith angles. For wavelengths longer than 305 nm, differences did not exceed 3%. Actinic flux and global irradiance values at the surface were underestimated in some cases up to 40% at 295 nm for 70° caused mainly due to ozone redistribution. Significant differences were calculated at 85° for higher UV-B wavelengths, while the increase of UV radiation in some cases could be attributed to the decreased temperature profile values. So, vertical profiles of ozone and

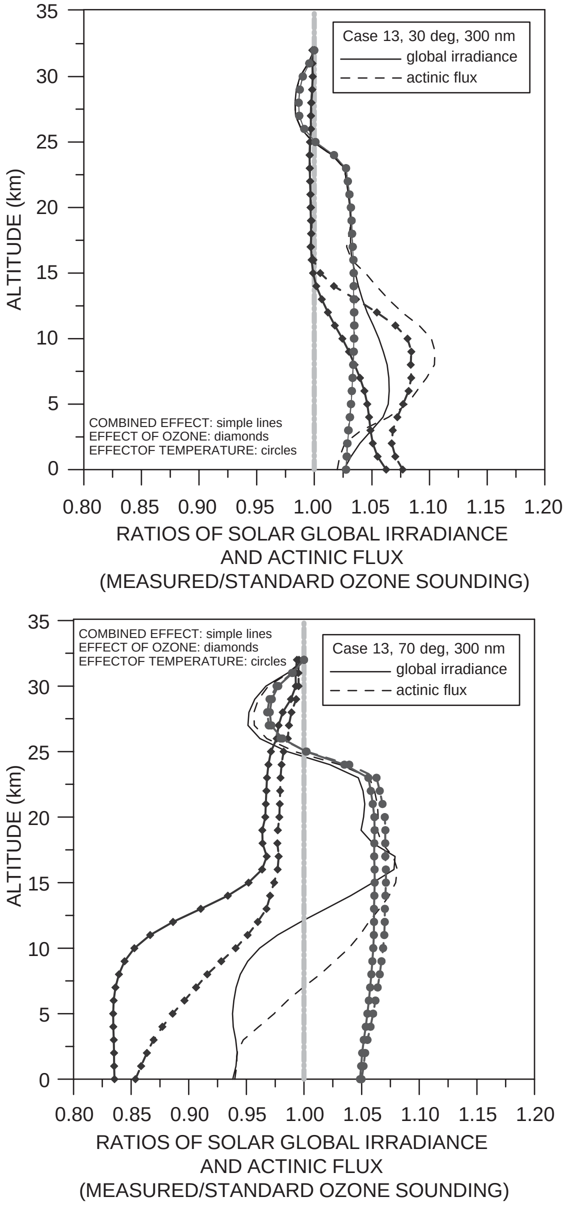


Fig. 6. Model calculated ratios of global solar irradiance and actinic flux for 300 nm with altitude using the measured and standard profiles of ozone and temperature at 30° (upper panel) and 70° (lower panel).

temperature may be well known for accurate spectral model calculations and comparison with ground-based measurements, especially at high solar zenith angles.

For UV-B and CIE erythemal doses model calculated differences did not exceed 2% and 3%, respectively for 30° and 70°. However, for 85° (where UV radiation is low), the use of measured profiles of ozone and temperature instead of standard AFGL profile leads to differences on integral values up to 20%.

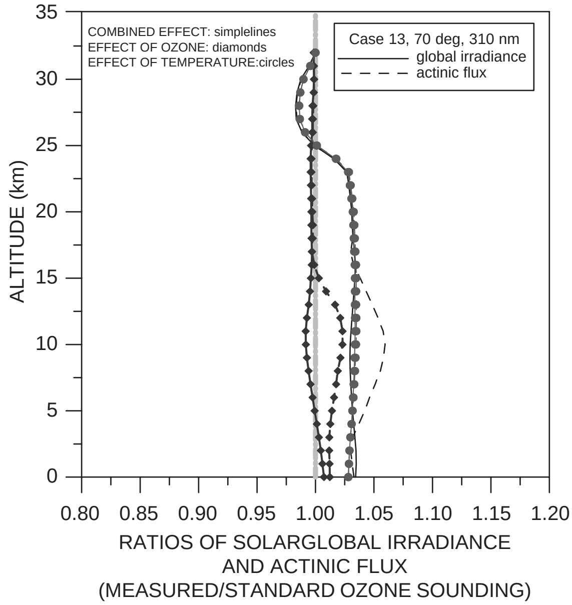


Fig. 7. Model calculated ratios of global solar irradiance and actinic flux for 310 nm with altitude using the measured and standard profiles of ozone and temperature at 70°.

A specific vertical ozone and temperature profile corresponding to polar air masses probed over Thessaloniki was selected as to examine the differences in the vertical distribution of UV radiation. The significant differences of temperature profile values with respect to the standard AFGL profile resulted in model calculated direct irradiance differences in the troposphere up to 10% for 70° but only 4% for 30°. Redistribution of ozone affects strongly global irradiance and actinic flux in the troposphere especially at the higher solar zenith angle. The above results show that for comparison of model calculated spectra with measurements at short UV-B wavelengths in the troposphere (from balloons, aircrafts, etc.) the choice of seasonal average ozone and temperature profiles for a given area must be carefully utilized for high solar zenith angles.

## Acknowledgement

This study was partly conducted in the framework of the project GR-UVNET, which was funded by the Greek Ministry of Commerce.

## References

Anderson G., Clough, S., Krneizys, F., Chetwynd, J., Shettle, A., 1986 AFGL atmospheric constituent profiles (0–120 km), Technical Report AFGL-Tr-86—110, Air

Force Geophys. Lab., Hanscom Air Force Base, Bedford, MA.

Bais, A.F., Zerefos, C.S., Meleti, C., Ziomas, I.C., Tourpali, C., 1993. Spectral measurements of solar UVB radiation and its relations to total ozone, $SO_2$ and clouds. Journal of Geophysical Research 98 (D3), 5199–5204.

Bais, A.F., Gardiner, B.G., Slaper, H., Blumthaler, M., Bernhard, G., Mckenzie, R.L., Webb, A.R., Seckmeyer, G., Kjeldstad, B., Koskela, T., Kirsch, P., Groebner, J., Kerr, J.B., Kazadzis, S., Lesczynski, K., Wardle, D., Brogniez, C., Josefsen, W., Gillotay, D., Reinen, H., Weihs, P., Svenoe, T., Eriksen, P., Kuik, F., Redondas, A., 2001. SUSPEN intercomparison of ultraviolet spectroradiometers. Journal of Geophysical Research 106 (D12), 12,509–12,526.

Bais, A.F., Madronich, S., Crawford, J., Hall, S.R., Mayer, B., van Weele, M., Lenoble, J., Calvert, J.G., Cantrell, C.A., Shetter, R.E., Hofzumahaus, A., Koepke, P., Monks, P.S., Frost, G., McKenzie, R., Krotkov, N., Kylling, A., Swartz, W.H., Lloyd, S., Pfister, G., Martin, T.J., Roeth, E.-P., Griffioen, E., Ruggaber, A., Krol, M., Kraus, A., Edwards, G.D., Mueller, M., Lefer, B.L., Johnston, P., Schwander, H., Flittner, D., Gardiner, B.G., Barrick, J., Schmitt, R., 2003. International photolysis frequency measurement and model intercomparison (IPMMI): spectral actinic solar flux measurements and modeling. Journal of Geophysical Research 108 (D16), 12.

Bais, A.F., Kazantzidis, A., Kazadzis, S., Balis, D.S., Zerefos, C.S., Meleti, C., 2004. Deriving an effective aerosol single scattering albedo from spectral surface UV irradiance measurements. Atmospheric Environment 39 (6), 1093–1102.

Balis, D.S., Zerefos, C.S., Kourtidis, K., Bais, A.F., Hofzumahaus, A., Kraus, A., Schmitt, R., Blumthaler, M., Gobbi, G.P., 2002. Measurements and modeling of photolysis rates during the photochemical activity and ultraviolet radiation (PAUR) II campaign. Journal of Geophysical Research 107 (D18), 8138.

Bass, A.M., Paur, R.J., 1985. The ultraviolet cross-section of ozone: I. The measurements. In: Zerefos, C.S., Ghazi, A. (Eds.), Atmospheric Ozone, Proceedings of the Quadrennial Ozone Symposium, Reidel Publication, Dordrecht, pp. 601–606.

Blumthaler, M., Ambach, W., 1988. Solar UVB-albedo of various surfaces. Photochemistry and Photobiology 48, 85–88.

Bruehl, C., Crutzen, P., 1989. On the disproportionate role of tropospheric ozone as a filter against solar UV-B radiation. Geophysical Research Letters 16, 703–706.

Dahlback, A., Stamnes, K., 1991. A new spherical model for computing the radiation field available for photolysis and heating at twilight. Planetary Space Science 39, 671–683.

De Backer, H., Koepke, P., Bais, A., de Cabo, X., Frei, T., Gillotay, D., Haite, C., Heikkila, A., Kazantzidis, A., Koskela, T., Kyrϕ, E., Lapeta, B., Lorente, J., Masson, K., Mayer, B., Plets, H., Redondas, A., Renaud, A., Schauberger, G., Schmalwieser, A., Schwander, H., Vanicek, K., 2001. Comparison of measured and modeled UV indices for the assessment of health risks. Meteorological Applications 8 (3), 267–277.

Elterman, L., 1968. UV, Visible and IR attenuation for altitudes to 50 km, AFCR-68-0153, Air Force Cambridge Research Laboratory, Bedford, MA.

Fioletov, V.E., Kerr, J.B., Wardle, D.I., 1997. The relationship between total ozone and spectral UV irradiance from Brewer observations and its use for derivation of total ozone from UV measurements. Geophysical Research Letters 24, 2997–3000.

Forster, P.M.de.F., 1995. Modeling ultraviolet radiation at the Earth's surface, Part I: the sensitivity of ultraviolet irradiances to atmospheric changes. Journal of Applied Meteorology 34, 2412–2425.

Galani, E., Balis, D., Zanis, P., Zerefos, C., Papayannis, A., Wernli, H., Gerasopoulos, E., 2003. Observations of stratosphere-to-troposphere transport events over the eastern Mediterranean using a ground-based lidar system. Journal of Geophysical Research 108 (D12), 8527.

Kazantzidis, A., Balis, D.S., Bais, A.F., Kazadzis, S., Galani, E., Kosmidis, E., Blumthaler, M., 2001. Comparison of model calculations with spectral UV measurements during the SUSPEN campaign: the effect of aerosols. Journal of Atmospheric Sciences 58, 1529–1539.

Kerr, R.A., McElroy, C.T., 1993. Evidence of Large upward trends of ultraviolet-B radiation linked to ozone depletion. Science 262, 1032–1034.

Kerr, J.B., Fast, H., McElroy, C.T., Oltmans, S.J., Lathrop, J.A., Kyro, E., Paukkunen, A., Claude, H., Koehler, U., Sreedharan, C.R., Takao, T., Tsukagoshi, Y., 1994. The 1991 WMO international ozonesonde intercomparison at Vanscoy, Canada. Atmosphere Ocean 32, 685–716.

Knudsen, B.M., Carver, G.D., 1994. Accuracy of the isentropic trajectories calculated for the EASOE campaign. Geophysical Research Letters 21, 1199–1202.

Koepke, P., Bais, A., Balis, D., Buchwitz, M., De Backer, H., de Cabo, X., Eckert, P., Eriksen, P., Gillotay, D., Heikkilä, A., Koskela, T., Lapeta, B., Litynska, Z., Lorente, J., Mayer, B., Renaud, A., Ruggaber, A., Schauberger, G., Seckmeyer, G., Seifert, P., Schmalwieser, A., Schwander, H., Vanicek, K., Weber, M., 1998. Comparison of models used for UV index calculations. Photochemistry and Photobiology 67, 657–662.

Kourtidis, K., Zerefos, C., Balis, D., Kosmidis, E., Rapsomanikis, S., Perros, P.E., Simeonov, V., Melas, D., Thompson, A., Witte, J., Calpini, B., Rappenglueck, B., Isaksen, I., Papayannis, A., Hofzumahaus, A., Gimm, H., Drakou, R., 2002. Regional tropospheric ozone over eastern Mediterranean. Journal of Geophysical Research 107 (D18), 8140.

Kylling, A., Mayer, B., 2001. Ultraviolet radiation in partly snow covered terrain: observations and three-dimensional simulations. Geophysical Research Letters 28, 3665–3668.

Kylling, A., Bais, A.F., Blumthaler, M., Schreder, J., Zerefos, C.S., Kosmidis, E., 1998. Effect of aerosols on solar UV irradiances during the photochemical activity and solar ultraviolet radiation campaign. Journal of Geophysical Research. 103, 26,051–26,060.

Kylling, A., Persen, T., Mayer, B., Svenoe, T., 2000a. Determination of an effective spectral surface albedo from ground-based global and direct UV irradiance measurements. Journal of Geophysical Research 105, 4949–4959.

Kylling, A., Dahlback, A., Mayer, B., 2000b. The effect of clouds and surface albedo on UV irradiances at a high latitude site. Geophysical Research Letters 27, 1411–1414.

Lapeta, B., Engelsen, O., Litynska, Z., Kois, B., Kylling, A., 2000. Sensitivity of surface UV radiation and ozone column retrieval to ozone and temperature profiles. Journal of Geophysical Research 105, 5001–5007.

Madronich, S., 1993. UV radiation in the natural and perturbed atmosphere. In: Tevini, M. (Ed.), Environmental Effects of Ultraviolet Radiation. Lewis Publisher, Boca Raton, pp. 17–69.

Mayer, B., Seckmeyer, G., Kylling, A., 1997. Systematic long-term comparison of spectral UV measurements and UVSPEC modeling results. Journal of Geophysical Research 102, 8755–8767.

Mayer, B., Fischer, C.A., Madronich, S., 1998. Estimation of surface actinic flux from satellite (TOMS) ozone and cloud reflectivity measurements. Geophysical Research Letters 25, 4321–4324.

McKenzie, R.L., Matthews, W.A., Johnston, P.V., 1991. The relationship between erythemal UV and ozone derived from spectral irradiance measurements. Geophysical Research Letters 18, 2269–2272.

McKenzie, R., Smale, D., Bodeker, G., Claude, H., 2003. Ozone profile differences between Europe and New Zealand: effects on surface UV irradiance and its estimation from satellite sensors. Journal of Geophysical Research 108 (D6), 4179.

McKinlay, A.F., Diffey, B.L., 1987. A rerference action spectrum for ultraviolet induced erythema in human skin. CIE Journal 6, 17–22.

Nicolet, M., 1984. On the molecular scattering in the terrestrial atmosphere: an empirical formula for its calculation in the homosphere. Planetary Space Science 32 (11), 1467–1468.

Rex, M., von der Gathen, P., Braathen, G.O., Harris, N.R.P., Reimer, E., Beck, A., Alfier, R., Krüger-Carstensen, R., Chipperfield, M., De Backer, H., Balis, D., O'Connor, F., Dier, H., Dorokhov, V., Fast, H., Gamma, A., Gil, M., Kyrö, E., Litynska, Z., Mikkelsen, I.S., Molyneux, M., Murphy, G., Reid, S.J., Rummukainen, M., Zerefos, C., 1999. Chemical ozone loss in the Arctic winter 1994/95 as determined by the match technique. Journal of Atmospheric Chemistry 32, 35–59.

Ruggaber, A., Dlugi, R., Nakajima, T., 1994. Modelling radiation quantities and photolysis frequencies in the troposphere. Journal of Atmospheric Chemistry 18, 171–210.

Schwander, H., Koepke, P., Ruggaber, A., 1997. Uncertainties in modeled UV irradiances due to limited accuracy and availability of input data. Journal of Geophysical Research 102, 9419–9429.

Stamnes, K.S., Tsay, C., Wiscombe, W., Jayaweera, K., 1988. Numerically stable algorithm for discrete-ordinate method radiative transfer in multiple scattering and emitting layered media. Applied Optics 27, 2502–2509.

Tsay, C., Stamnes, K.S., 1992. Ultraviolet radiation in the Arctic: the impact of potential ozone depletions and cloud effects. Journal of Geophysical Research 97, 7829–7840.

Weihs, P., Webb, A.R., 1997a. Accuracy of spectral UV model calculations, 2, comparison of UV calculations with measurements. Journal of Geophysical Research 102, 1551–1560.

Weihs, P., Webb, A.R., 1997b. Accuracy of spectral UV model calculations, 1, consideration of uncertainties in input parameters. Journal of Geophysical Research 102, 1541–1550.

World Meteorological Organization, 1998. Scientific assesment of ozone depletion, WMO Report 44.

Zeng, J., McKenzie, R., Stamnes, K., Wineland, W., Rosen, J., 1994. Measured UV spectra compared with discrete ordinate method simulations. Journal of Geophysical Research 99, 23,019–23,030.

Zerefos, C.S., Balis, D.S., Bais, A.F., Gillotay, D., Simon, P.C., Mayer, B., Seckmeyer, G., 1997. Variability of UV-B at four stations in Europe. Geophysical Research Letters 24, 1363–1366.

Zerefos, C., Meleti, C., Balis, D., Tourpali, K., Bais, A.F., 1998. Quasi-biennial and longer-term changes in clear sky UV-B solar irradiance. Geophysical Research Letters 25, 4345–4348.

Zerefos, C.S., Kourtidis, K.A., Melas, D., Balis, D., Zanis, P., Mantis, H.T., Repapis, C., Isaksen, I., Sundet, J., Herman, J., Bhartia, P.K., Calpini, B., 2002. Photochemical activity and solar ultraviolet radiation modulation factors (PAUR): an overview of the project. Journal of Geophysical Research.